Available online at www.sciencedirect.com
ScienceDirect
Polymer 48 (2007) 195–204
polymer
www.elsevier.com/locate/polymer

Freezing as a path to build macroporous structures: Superfast responsive polyacrylamide hydrogels

M. Valentina Dinu [a], M. Murat Ozmen [b], E. Stela Dragan [a], Oguz Okay [b,*]

[a] "Petru Poni" Institute of Macromolecular Chemistry, Functional Polymers Department, Iasi, Romania
[b] Istanbul Technical University, Department of Chemistry, Maslak 34469, Istanbul, Turkey

Received 5 October 2006; received in revised form 7 November 2006; accepted 11 November 2006
Available online 1 December 2006

Abstract

Macroporous polyacrylamide (PAAm) hydrogels were prepared from acrylamide monomer and *N*,*N*′-methylene(bis)acrylamide (BAAm) crosslinker in frozen aqueous solutions. It was found that the swelling properties and the elastic behavior of the hydrogels drastically change at a gel preparation temperature of −6 °C. The hydrogels prepared below −6 °C exhibit a heterogeneous morphology consisting of pores of sizes 10–70 μm, while those formed at higher temperatures have a non-porous structure. PAAm networks with largest pores were obtained at −18 °C. The pore size of the networks increased while the thickness of the pore walls decreased by decreasing the monomer concentration. The hydrogels formed below −6 °C exhibit superfast swelling and deswelling properties as well as reversible swelling–deswelling cycles in water and in acetone, respectively.

Keywords: Macroporous hydrogels; Freezing; Swelling

1. Introduction

Responsive hydrogels are soft and smart materials, capable of changing volume and/or shape in response to specific external stimuli, such as the temperature, solvent quality, pH, electric field, etc. [1]. Depending on the design of the hydrogel matrices, this volume change may occur continuously over a range of stimulus values, or, discontinuously at a critical stimulus level. These properties of the hydrogels received considerable interest in last three decades and, a large number of hydrogel-based devices have been proposed, including artificial organs, actuators, and on-off switches. However, the practical design and control of these devices still present some problems. In particular, hydrogel-based devices are limited in their response rate by diffusion processes, which are slow and even slower near the critical point [2]. In order to increase the response rate of hydrogels, several techniques were proposed, such as reducing the size of the gel particles [3], creating dangling chains on the gel samples [4], or, constructing an interconnected pore structure within the hydrogel matrices [5].

As is well known, in sea ice, pure hexagonal ice crystals are formed and the various impurities, e.g., salts, biological organisms, etc. are expelled from the forming ice and entrapped within the liquid channels between the ice crystals [6,7]. This natural principle was used by Lozinsky for the preparation of porous gels [8]. As in nature, during the freezing of a monomer solution, the monomers expelled from the ice concentrate within the channels between the ice crystals, so that the polymerization reactions only take place in these unfrozen liquid channels. After polymerization and, after melting of ice, a porous material is produced whose microstructure is a negative replica of the ice formed [9–12]. Recently, we have shown that by conducting the copolymerization–crosslinking reactions below −8 °C, hydrogels based on 2-acrylamido-2-methylpropane sulfonic acid (AMPS) monomer with superfast swelling properties could be

* Corresponding author. Tel.: +90 212 2853156; fax: +90 212 2856386.
E-mail address: okayo@itu.edu.tr (O. Okay).

0032-3861/$ - see front matter © 2006 Elsevier Ltd. All rights reserved.
doi:10.1016/j.polymer.2006.11.022

obtained [13]. This was achieved by using gelation reactions occurring in the apparently frozen reaction system, which allowed for the formation of a bicontinuous morphology in poly(AMPS) (PAMPS) networks. It was shown that the free water freezing in the gel causes the network chains to gather and condense so that a heterogeneous network forms after removing the ice [13]. The PAMPS network maintains a honeycomb structure upon drying.

In this report, we apply this procedure for the preparation of polyacrylamide (PAAm) hydrogels. The copolymerization–crosslinking reactions of acrylamide (AAm) monomer and *N*,*N*′-methylenebis(acrylamide) (BAAm) crosslinker were carried out in aqueous solutions. We systematically varied the gel preparation temperature, the initial monomer concentration as well as the crosslinker content of the monomer mixture in order to obtain the optimum reaction conditions for the preparation of fast responsive PAAm hydrogels with a two-phase morphology. As will be seen below, PAAm hydrogels prepared below −6 °C swell immediately upon contact with water, regardless of their crosslinker contents. The size-independent superfast swelling and deswelling kinetics of the hydrogels is accounted for by their interconnected pore structure which is stable against the volume changes.

2. Experimental section

2.1. Materials

Acrylamide (AAm, Merck), *N*,*N*′-methylenebis(acrylamide) (BAAm, Merck), ammonium persulfate (APS, Merck), and *N*,*N*,*N*′,*N*′-tetramethylethylenediamine (TEMED, Merck) were used as received. Stock solutions of APS and TEMED were prepared by dissolving 0.16 g of APS and 0.50 mL of TEMED each in 20 mL of distilled water. Stock solution of BAAm was prepared by dissolving 0.132 g of BAAm in 10 mL of distilled water.

Polyacrylamide (PAAm) hydrogels were prepared by free-radical crosslinking–copolymerization of AAm with BAAm in aqueous solution at various temperatures (T_{prep}) between −25 °C and +25 °C. The initial concentration of the monomer (AAm + BAAm), C_o, as well as the crosslinker ratio X, which is the mole ratio of the crosslinker BAAm to the monomer AAm, was also varied in our experiments. The reaction time was set to 24 h. APS (3.51 mM) and TEMED (0.25 mL/100 mL reaction solution) were used as the redox initiator system. To illustrate the synthetic procedure, we give details for the preparation of hydrogels at $C_o = 5$ w/v% and $X = 1/80$.

AAm (0.4868 g), stock solutions of BAAm (1 mL), TEMED (1 mL), and distilled water (7 mL) were first mixed in a graduated flask of 10 mL in volume. The solution was cooled to 0 °C in ice-water bath, purged with nitrogen gas for 20 min and then, APS stock solution (1 mL) was added. Portions of this solution, each 1.5 mL, were transferred to glass tubes of 4 mm in diameter; the glass tubes were sealed, immersed in a thermostated bath at T_{prep} and the polymerization was conducted for one day. After polymerization, the gels were cut into specimens of approximately 10 mm in length and immersed in a large excess of water to wash out any soluble polymers, unreacted monomers and the initiator.

2.2. Methods

For the equilibrium swelling measurements, hydrogel samples after preparation in the form of rods of 4 mm in diameter and about 10 mm length were placed in an excess of water at room temperature (21 ± 0.5 °C). In order to reach swelling equilibrium, the hydrogels were immersed in water for at least two weeks replacing the water every other day. The swelling equilibrium was tested by measuring the diameter of the gel samples by using an image analyzing system consisting of a microscope (XSZ single Zoom microscope), a CDD digital camera (TK 1381 EG) and a PC with the data analyzing system Image-Pro Plus. The swelling equilibrium was also tested by weighing the gel samples. Thereafter, the equilibrium swollen hydrogel samples in water were carefully deswollen in a series of water–acetone mixtures with increasing acetone contents. This solvent exchange process facilitated final drying of the hydrogel samples. They were then washed several times with acetone and dried at 80 °C to constant weight. The equilibrium volume and the equilibrium weight swelling ratios of the hydrogels, q_v and q_w, respectively, were calculated as

$$q_v = \left(D_w/D_{dry}\right)^3 \tag{1a}$$

$$q_w = \left(m_w/m_{dry}\right) \tag{1b}$$

where D_w and D_{dry} are the diameters of the equilibrium swollen and dry gels, respectively, m_w and m_{dry} are the weight of gels after equilibrium swelling in water and after drying, respectively.

For the deswelling kinetics measurements, the equilibrium swollen hydrogel samples in water were immersed in acetone at 21 °C. The weight changes of the gels were measured gravimetrically after blotting the excess surface solvent at regular time intervals. For the measurement of the swelling kinetics of gels, the collapsed gel samples in acetone were transferred into water at 21 °C. The weight changes of gels were also determined gravimetrically as described above. The results were interpreted in terms of the relative weight swelling ratio $m_{rel} = m/m_w$, where m is the mass of the gel sample at time t. The swelling kinetics measurements were also conducted in situ by following the diameter of the hydrogel samples under microscope using the image analyzing system mentioned above.

Uniaxial compression measurements were performed on equilibrium swollen gels in water. All the mechanical measurements were conducted in a thermostated room of 21 ± 0.5 °C. The stress–strain isotherms were measured by using an apparatus previously described [14]. Briefly, a cylindrical gel sample of 4–8 mm in diameter and 7–15 mm in length was placed on a digital balance (Sartorius BP221S, readability and reproducibility: 0.1 mg). A load was transmitted vertically to the gel through a rod fitted with a PTFE end-plate. The compressional force acting on the gel was calculated from the readings in the

balance. The resulting deformation was measured after 20 s of relaxation by using a digital comparator (IDC type Digimatic Indicator 543-262, Mitutoyo Co.), which was sensitive to displacements of 10^{-3} mm. The measurements were conducted up to about 15% compression. From the repeated measurements, the standard deviations in the modulus value were less than 3%. The sample weight loss during the measurements due to water evaporation was found to be negligible. The elastic modulus G was determined from the slope of linear dependence [15],

$$f = G\left(\lambda - \lambda^{-2}\right) \tag{2}$$

where f is the force acting per unit cross-sectional area of the undeformed gel specimen, and λ is the deformation ratio (deformed length/initial length).

For the texture determination of dry hydrogels, scanning electron microscopic studies were carried out at various magnifications between 50 and 300 times (Jeol JSM 6335F Field Emission SEM). Prior to the measurements, network samples were sputter-coated with gold for 3 min using Sputter-coater S150 B Edwards instrument. The texture of the dry hydrogels was also investigated under XSZ single Zoom microscope using the image analyzing system Image-Pro Plus.

The dry-state porosity of the networks was estimated from their densities. For this purpose, the weight m_{dry} and the dimensions (diameter D_{dry} and length l_{dry}) of cylindrical PAAm network samples were measured, from which their densities were calculated as $m_{dry}/(\pi D_{dry}^2 l_{dry}/4)$. The total porosity P was calculated as

$$P = (1 - d_0/d_2) \tag{3}$$

where d_0 and d_2 are the densities of porous and non-porous networks.

The pore volume V_p of the networks was estimated through uptake of cyclohexane of dry hydrogels. Since cyclohexane is a non-solvent for PAAm, it only enters into the pores of the polymer networks. Thus, V_p (mL pores in 1 g of dry polymer network) was calculated as

$$V_p = \left(m_{CH} - m_{dry}\right)/\left(d_{CH} m_{dry}\right) \tag{4}$$

where m_{CH} is the weight of the network immersed in cyclohexane after 48 h and d_{CH} is the density of cyclohexane.

For the determination of the non-freezable water content of the hydrogels, DSC measurements were carried out on Perkin–Elmer Diamond DSC. Equilibrium swollen PAAm hydrogels in water were placed in an aluminum sample pan of the instrument. The pan with swollen gel was sealed and weighed. Then, it was frozen within the instrument at various temperatures and then heated to 60 °C with a scanning rate of 2.5 °C/min. The transition enthalpy ΔH for the melting of frozen water was determined. After the scans, the pans were punctured and dried at 80 °C to constant weight. The total water content of the hydrogel m_{water} was calculated as $m_{water} = m_1 - m_2$, where m_1 is the weight of the pan with swollen gel and m_2 is the same weight but after drying. The mass fraction of non-freezable water in the gel, f_{H_2O} was calculated as

$$f_{H_2O} = 1 - (\Delta H/\Delta H_m)/m_{water} \tag{5}$$

where ΔH_m is the heat of melting of ice which is 334.45 J/g. It should be noted that the reorganization of the water molecules in the frozen hydrogel samples and the associated heat effects were neglected in the derivation of Eq. (5) [16,17].

3. Results and discussion

Three sets of gelation experiments were carried out (Table 1). In the first set, the gel preparation temperature, T_{prep}, was varied between −25 and 25 °C. In the second set, T_{prep} was set to −18 °C while the initial monomer concentration C_o was varied between 2 and 30 w/v%. In the third set, the crosslinker ratio X was varied over a wide range at $T_{prep} = -18$ °C. The monomer conversion (mass of crosslinked polymer/initial mass of the monomer) was found to be larger than 90% in all the experiments.

Results of the elasticity measurements with hydrogels obtained from the three sets of experiments are summarized in Fig. 1A–C, respectively. Here, the elastic moduli G of the equilibrium swollen hydrogels in water are plotted against the gel preparation temperature T_{prep} (A), the initial monomer concentration C_o (B), and the crosslinker ratio X (C). Depending on T_{prep}, two different regimes can be seen from Fig. 1A. At $T_{prep} = -6$ °C or above, the gels exhibit a relatively low modulus of elasticity around 1500 Pa. However, decreasing T_{prep} below −6 °C results in a fourfold increase in the elastic modulus of the gels. The transition between the two regimes is shown in the figure by the vertical dashed line. Moreover, the gels formed at or above −6 °C were transparent while those formed at lower temperatures were opaque, indicating that these gels have separate domains in a spatial scale of submicrometer to micrometer. Thus, the hydrogel properties drastically change as T_{prep} is decreased below −6 °C. Fig. 1A also shows that, for T_{prep} below −6 °C, the elastic modulus decreases as the temperature is further decreased. This is probably due to the decrease of the crosslinking efficiency by reducing the polymerization temperature so that the gels formed at lower temperature exhibit lower moduli of elasticity. Fig. 1B shows that, increasing initial monomer concentration C_o from 3 to 30 w/v% results in two orders of magnitude increase in the modulus of the hydrogels. Indeed, hydrogels formed at $C_o = 3\%$ or below were too weak to withstand the mechanical tests while those formed at or above 10% monomer concentration were highly stable against the

Table 1
The three sets of experiments conducted at various reaction conditions

Code	T_{prep} (°C)	C_o (w/v%)	X ([BAAm]/[AAm])
1	−25 → +25	5	1/80
2	−18	2 → 30	1/80
3	−18	3	1/5 → 1/100

C_o = initial monomer concentration, X = the crosslinker ratio, i.e., the molar ratio of the crosslinker BAAm to the monomer AAm, and T_{prep} = gel preparation temperature.

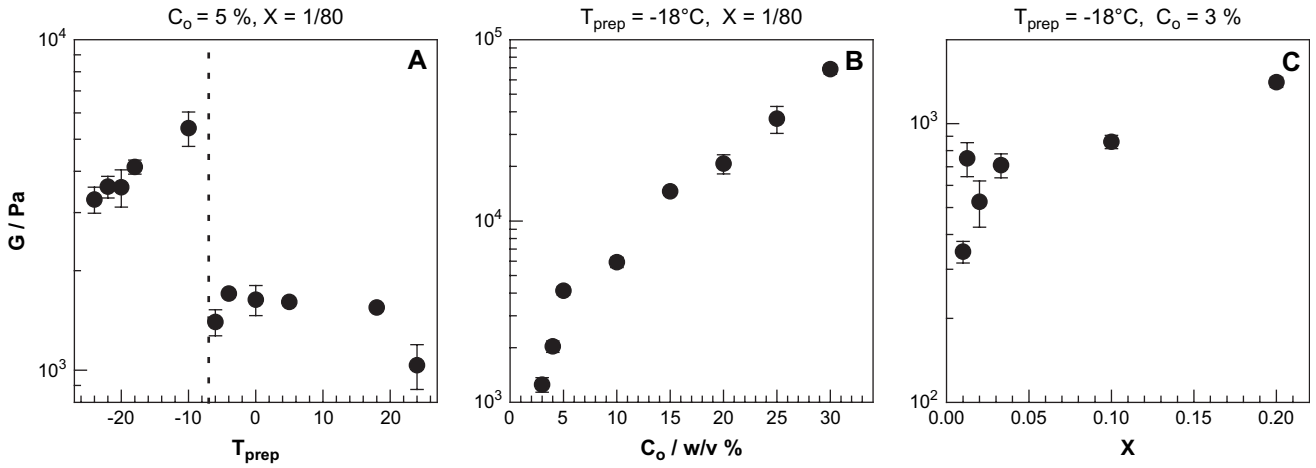

Fig. 1. The elastic modulus G of equilibrium swollen PAAm hydrogels shown as functions of the gel preparation temperature T_{prep} (A), the initial monomer concentration C_o (B), and the crosslinker ratio X (C).

mechanical forces. They were very tough and could withstand high levels of deformation such as elongation, bending, and compression; in the equilibrium swollen state, they can be squeezed completely between the fingers without an irreversible deformation of the main shape or without breaking. In contrast to the effect of C_o, the increase of the crosslinker ratio X from 1/100 to 1/5 did not result in a significant increase in the modulus of hydrogels (Fig. 1C).

The relative values of the weight and the volume swelling ratios of the hydrogels provide information about their internal structure in the swollen state [5]. During the swelling process, the pores inside the network are rapidly filled with the solvent; at the same time, the polymer region takes up solvent from the environment whose extent depends on the attractive force between the solvent molecules and polymer segments. Thus, two separate processes govern the swelling of porous networks:

(a) solvation of network chains,
(b) filling of the pores by the solvent.

The equilibrium weight swelling ratio q_w includes the amount of solvent taken by both of these processes, i.e., q_w includes the solvent in the gel as well as in the pore regions of the network. Thus, both the solvation and filling processes are responsible for the q_w values of the networks. On the contrary, if we assume isotropic swelling, that is the volume of the pores remains constant upon swelling, volume swelling ratio q_v of porous networks is caused by solvation of the network chains, i.e., by the first process. Thus, q_v only includes the amount of solvent taken by the gel portion of the network. Accordingly, the higher the difference between q_w and q_v, the higher is the volume of the pores in the network sample. In Fig. 2A–C, the equilibrium weight (q_w, filled symbols) and the equilibrium volume swelling ratios (q_v, open symbols) of the hydrogels are shown as functions of the experimental parameters T_{prep}, C_o, and X. For the hydrogels formed at or above -6 °C, both q_w and q_v equal to 20–23, and they are independent of T_{prep}. However, as T_{prep} is decreased below -6 °C, the volume swelling ratio rapidly decreases and at $T_{prep} < -10$ °C, the hydrogels swell about sixfold more by weight than by volume. These

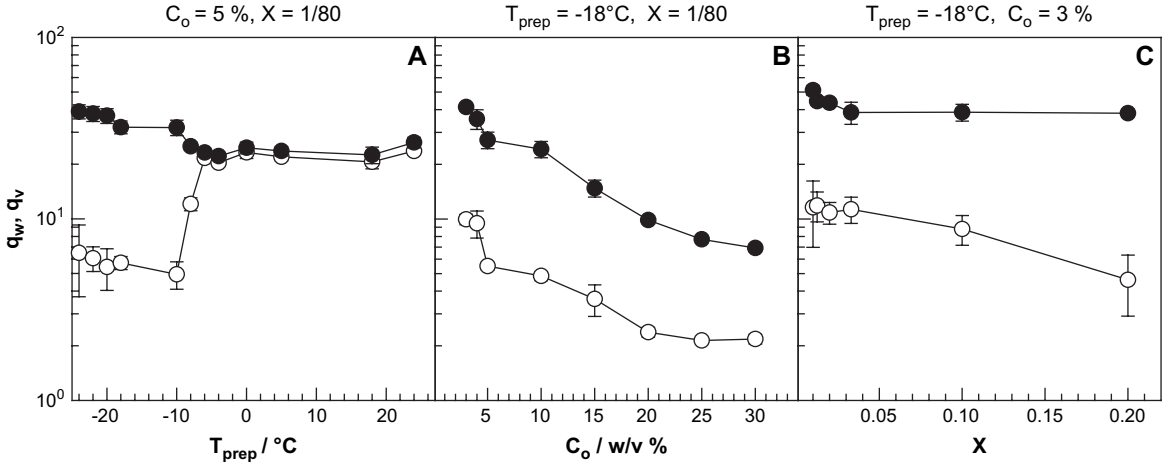

Fig. 2. The equilibrium weight (q_w, filled symbols) and the equilibrium volume swelling ratios (q_v, open symbols) of the hydrogels shown as functions of the experimental parameters T_{prep}, C_o, and X.

results suggest appearance of pores in the hydrogel matrices prepared at $T_{prep} < -6$ °C. Moreover, Fig. 2B and C shows that, over the entire range of the initial monomer concentration C_o and the crosslinker ratio X, the weight swelling ratio of the hydrogels is also much larger than their volume swelling ratio. Both q_w and q_v decrease as the monomer concentration or the crosslinker ratio is increased.

From the weight and volume swelling ratios of hydrogels, the swollen state porosity of the networks P_s can be estimated using the equation [5,18,19]:

$$P_s = 1 - q_v[1 + (q_w - 1)d_2/d_1]^{-1} \quad (6)$$

where d_1 and d_2 are the densities of solvent (water) and polymer, respectively. Assuming that $d_1 = 1$ g/mL and $d_2 = 1.35$ g/mL [20], we calculated swollen state porosities P_s of the networks by use of Eq. (6). The results are shown in Fig. 3A–C by the open circles plotted against T_{prep}, C_o, and X. The swollen state porosity P_s is about 30% for the hydrogels formed at $T_{prep} \geq -6$ °C while it rapidly increases with decreasing T_{prep} below -6 °C and becomes close to 90% at $T_{prep} < -10$ °C. Moreover, P_s is about 80% for all the hydrogels prepared in the second and third sets of experiments. The filled circles in the figures represent the dry-state porosities P of the networks calculated from the polymer densities together with Eq. (3).

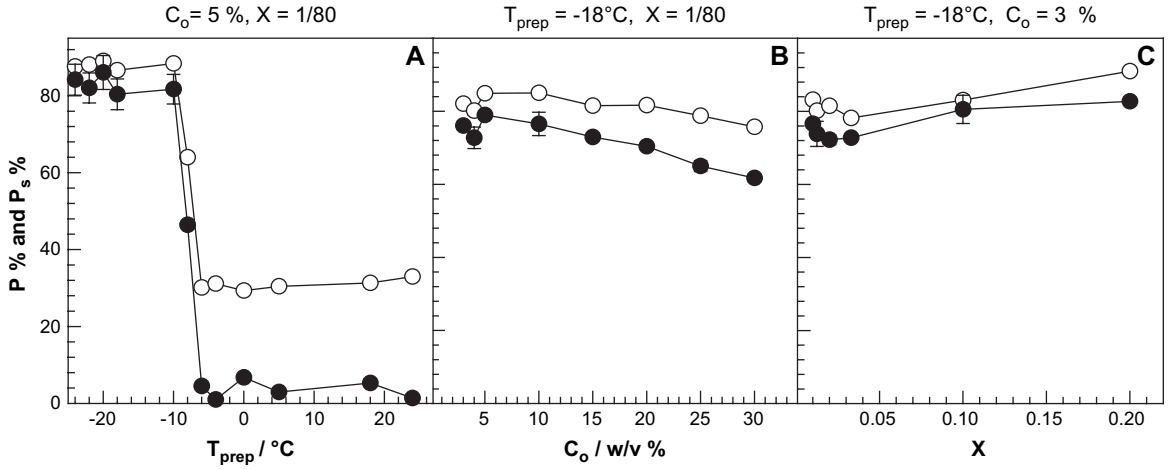

Fig. 3. The swollen state porosity P_s (open circles) and the dry-state porosity P of the networks (filled circles) plotted against the gel preparation temperature T_{prep} (A), the initial monomer concentration C_o (B), and the crosslinker ratio X (C).

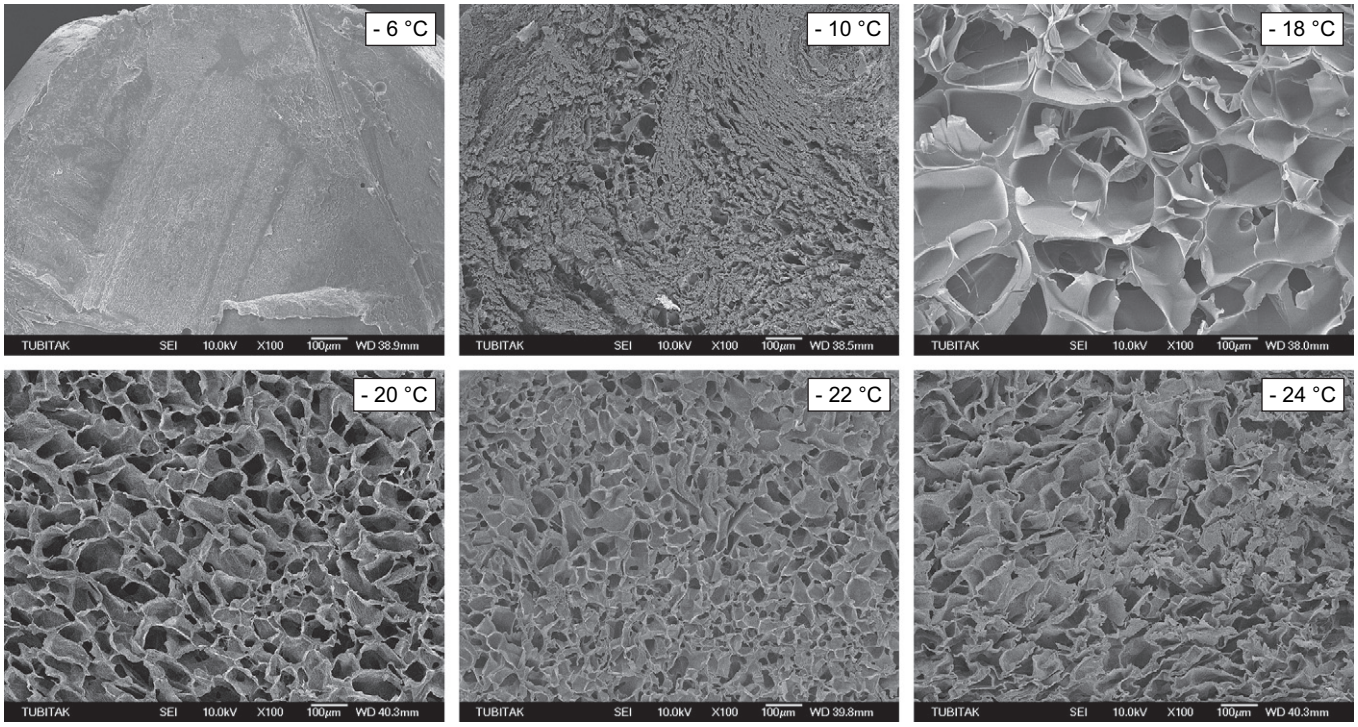

Fig. 4. SEM images of PAAm networks formed at various T_{prep} indicated in the figures. $C_o = 5$ w/v%, $X = 1/80$. The scaling bars are 100 μm. Magnification = ×100.

Interestingly, the two different techniques to estimate the porosity of the networks, namely one starting from the swelling ratios and the other from the polymer densities gave similar results. The dry-state porosity P is slightly lower than the swollen state porosity P_s, probably due to the partial collapse of the pores during drying. For hydrogels prepared at or above −6 °C, dry-state porosity is almost zero, i.e., the swollen state porosity totally disappears probably due to the collapse of the weak pore structure during drying. The total volume of pores, V_p, of the hydrogels was estimated from the uptake of cyclohexane. V_p was found to be in the range of 3–6 mL/g for the hydrogels prepared below −6 °C, while those formed at higher temperatures exhibited negligible pore volumes.

The morphologies of dried gel samples were observed both by scanning electron microscopy (SEM) and by the optical microscopy. SEM analysis of the networks formed below −6 °C revealed the presence of bicontinuous morphologies. In the scanning electron micrograph in Fig. 4, the microstructure of the network formed at various T_{prep} is given. Although the geometry and size of the pores are quite irregular, one can identify from Fig. 4 the regular assembly of polyhedral pores. This type of a microstructure is distinctly different from the macroporous networks formed by the reaction-induced phase separation mechanism, where the structure looks like cauliflower and consists of aggregates of various sizes [5]. All the polymer samples formed below −6 °C have a porous structure with pore diameters of 10–70 μm while those formed at or above −6 °C exhibit a continuous morphology. At −10 °C, the pore walls seem to be too weak so that they are more or less fused together to form large aggregates. Comparison of Figs. 1A and 2A with Fig. 4 indicates that the drastic change of the network microstructure between $T_{prep} = -6$ °C and −10 °C is reflected by the swelling and elasticity tests with decreasing volume swelling ratio (Fig. 2A) and increasing modulus of elasticity (Fig. 1A).

Fig. 4 also shows that the largest pore size was obtained at $T_{prep} = -18$ °C while it decreases as T_{prep} is further reduced up to −24 °C. The variation of the pore size depending on T_{prep} is also seen in Fig. 5 where the images taken from the optical microscope are shown. Note that the investigation of the network morphology under the optical microscope required no sample preparation. Cutting the hydrogel samples into thin slices prior to their drying was sufficient to obtain a large number of images. Since a statistical analysis of the pore structure was also possible using the image analyzing system, we estimated the pore sizes from the images taken from the microscope. By measuring the diameter of at least 30 pores, we calculated the average pore diameters as 60, 32, and 22 μm for $T_{prep} = -18$, −20, and −22 °C, respectively. Although the pore size varies depending on T_{prep}, the thickness of the pore walls was found to be constant at 4–5 μm.

The influence of monomer concentration on the network structure was also studied. In the SEM images in Fig. 6, the microstructure of the network formed at various concentrations C_o is given. It is observed that the architecture or morphology of the network essentially does not depend on the monomer concentration, whereas the size of the structure responds sensitively: the higher the monomer concentration, the smaller the pore diameters and the thicker the pore walls. The variation of the size of the structure depending on C_o is also seen in Fig. 7 where the images taken from the microscope are shown for the

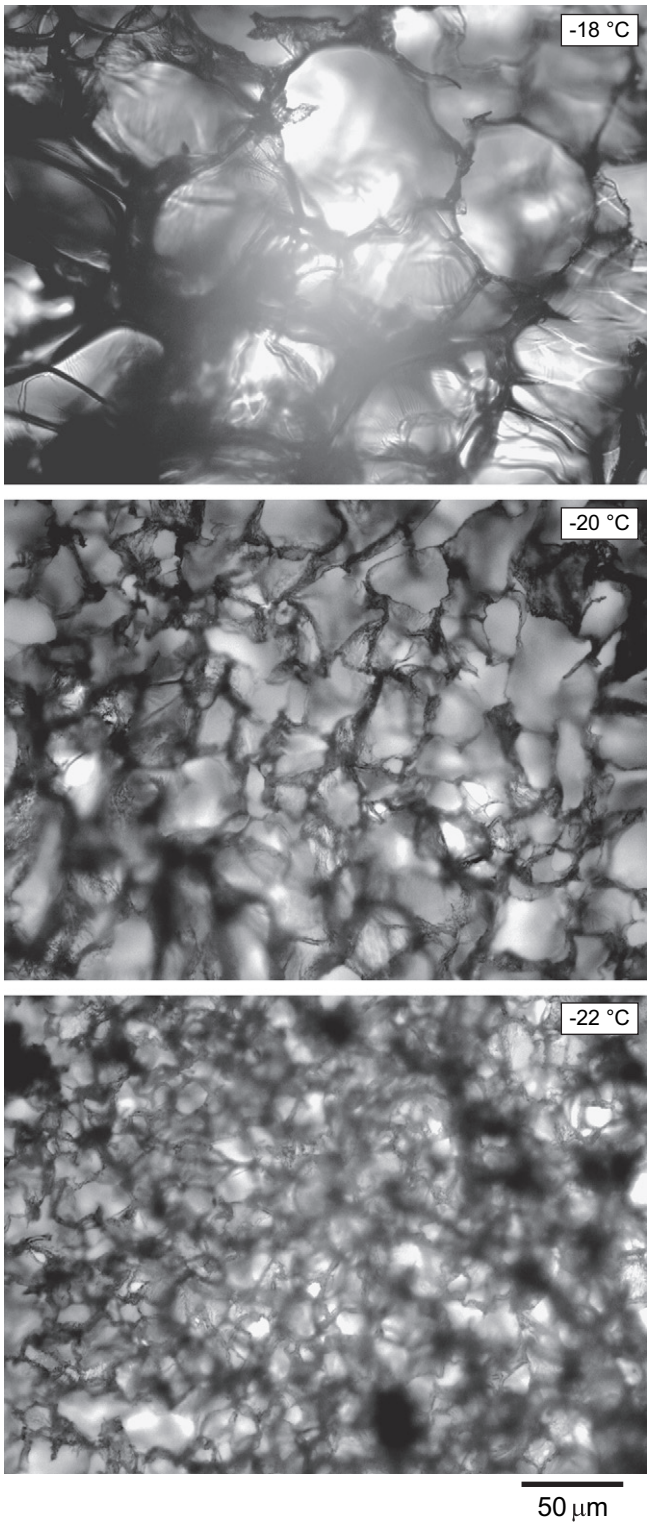

Fig. 5. Images taken from the optical microscope of the network samples prepared at various T_{prep} indicated in the figures. $C_o = 5$ w/v%, $X = 1/80$. The scaling bar is 50 μm.

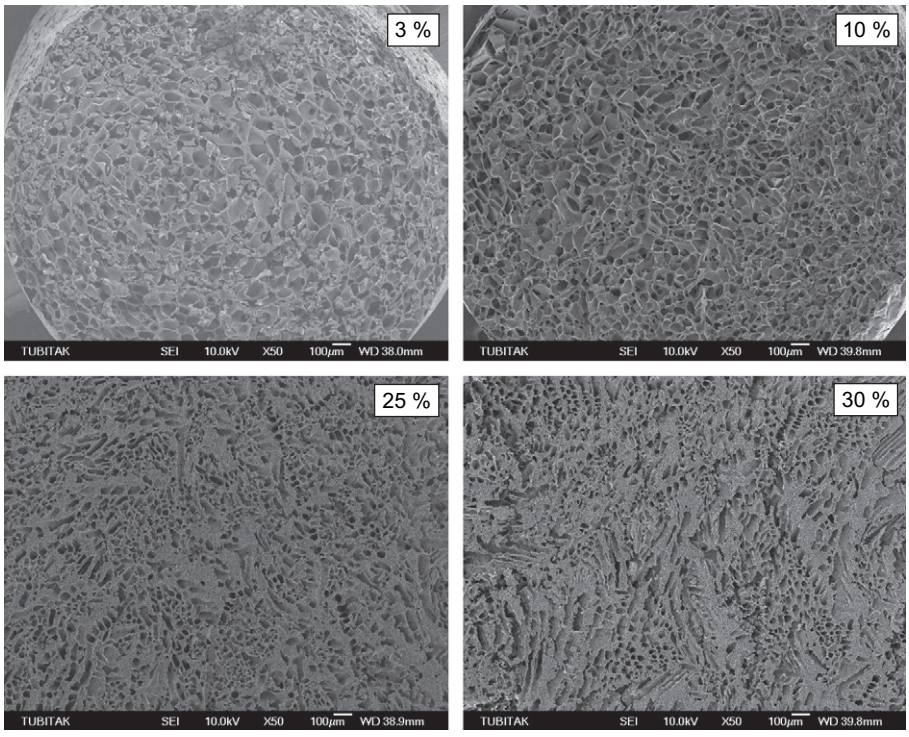

Fig. 6. SEM images of PAAm networks formed at various C_o indicated in the figures. $T_{prep} = -18\ ^\circ C$, $X = 1/80$. The scaling bars are 100 μm. Magnification = ×50.

dry networks prepared at $C_o = 3\%$ and 10%. After analyzing the whole network samples prepared at various C_o, the average pore diameter was found to decrease from 55 up to 10 μm with increasing C_o from 3% to 30%. At the same time, the average thickness of the pore walls increased from 3 to 15 μm. In PAAm gels with functional epoxy groups, Plieva et al. also reported decreasing pore size but increasing thickness of pore walls with increasing monomer concentration from 6% to 22% at $T_{prep} = -12\ ^\circ C$ [21]. In contrast, however, increasing pore size with increasing concentration was reported for PAMPS hydrogels obtained at $T_{prep} = -22\ ^\circ C$ [22]. For the third series, i.e., in the series in which the crosslinker ratio X was varied, no appreciable change in the size of the pores or pore walls was observed.

The occurrence of the polymerization and crosslinking reactions below the freezing point of water as well as the formation of a macroporous structure can be explained with the presence of unfrozen regions in the apparently frozen reaction system, in which the reactions proceed. To demonstrate that some water in the reaction system remains unfrozen even when cooled below the bulk freezing temperature, we conducted DSC measurements with frozen hydrogel samples from the first set of experiments. It was found that the apparently frozen hydrogel samples between −10 and −24 °C contain non-freezable water. The mass fraction of non-freezable water, f_{H_2O}, was found to be 0.06 ± 0.03, indicating that about 6% of water in the hydrogels which is bound to the polymer chains remains unfrozen even at −24 °C. Thus, the reactions

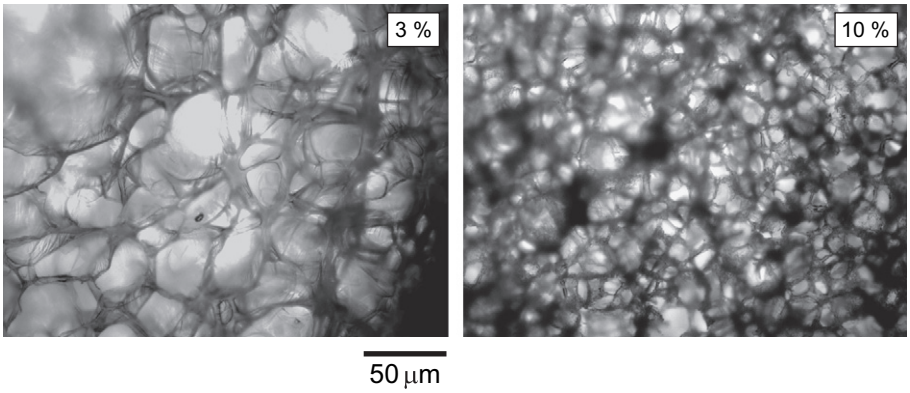

Fig. 7. Images taken from the optical microscope of the network samples prepared at two different C_o indicated in the figures. $T_{prep} = -18\ ^\circ C$, $X = 1/80$. The scaling bar is 50 μm.

only proceed in these unfrozen zones and lead to the formation of a polymer network with macroporous channels. The reason why water does not freeze below the bulk freezing temperature is attributed, in the main, to the freezing point depression of the water due to the solutes [23–25]. Although the usual solute concentrations can lower the freezing point by only a few degrees, once ice is present, the effect is enhanced. This is because solutes are excluded from the ice structure and become more concentrated in the remaining unfrozen regions. Thus, as water freezes (crystallizes), the solute concentration in the liquid phase rises continuously so that successively greater osmotic pressure is required to keep the liquid phase in equilibrium with the pure ice phase.

PAAm hydrogels thus obtained under various reaction conditions were subjected to swelling and deswelling processes in water and in acetone, respectively. For this purpose, the equilibrium swollen hydrogel in water was immersed in acetone and the weight change of gel was determined as a function of the deswelling time. After reaching the equilibrium collapsed state in acetone, the collapsed hydrogel was immersed in water and the swelling process was monitored by recording the weight increase with time. In order to check the durability of the gel sample against the volume changes, this swelling–deswelling cycle was repeated twice. Typical results are shown in Fig. 8 where the relative swelling ratio m_{rel} is plotted against the time of deswelling or swelling for the three series of gels. The filled symbols represent the hydrogels formed at −18 °C under various reaction conditions while open symbols represent the conventional hydrogels formed at 21 °C. It is seen that all the hydrogels prepared at −18 °C attain their equilibrium swollen and equilibrium collapsed states in less than 1 min and in 15 min, respectively, while those formed at higher temperatures require about 3 h to reach their equilibrium state in water. Similar results were also found for all the hydrogel samples prepared below −6 °C. Moreover, hydrogels formed below −6 °C also exhibited completely reversible swelling–deswelling cycles. However, those formed at higher temperatures exhibited irreversible cycles. For example, after the first deswelling process in acetone, the initial swollen mass of these hydrogels cannot be recovered in the following cycles (Fig. 8). The accelerating swelling and deswelling rates of gels prepared below $T_{prep} = -6$ °C are due to the formation of a porous structure in the networks, which increases their internal surface area so that the contact area between the solvent and the polymer increases. Thus, decreasing T_{prep} below −6 °C results in the formation of superfast responsive hydrogels, which are also stable against the volume changes.

It should be pointed out that, although the collapsed hydrogels prepared below −6 °C swell in water within 1 min (Fig. 8), the swelling of the same hydrogels starting from their dry states occurred immediately. For example, the pictures in the upper row of Fig. 9 were taken during the swelling process of a hydrogel sample formed at $T_{prep} = -18$ °C, $C_o = 5\%$, and $X = 1/80$. Starting from the dry state, the hydrogel attains its equilibrium swollen state in water within 4 s. Moreover, after swelling, if the gel sample is squeezed between the fingers completely (last picture in the upper row of Fig. 9), and immersed

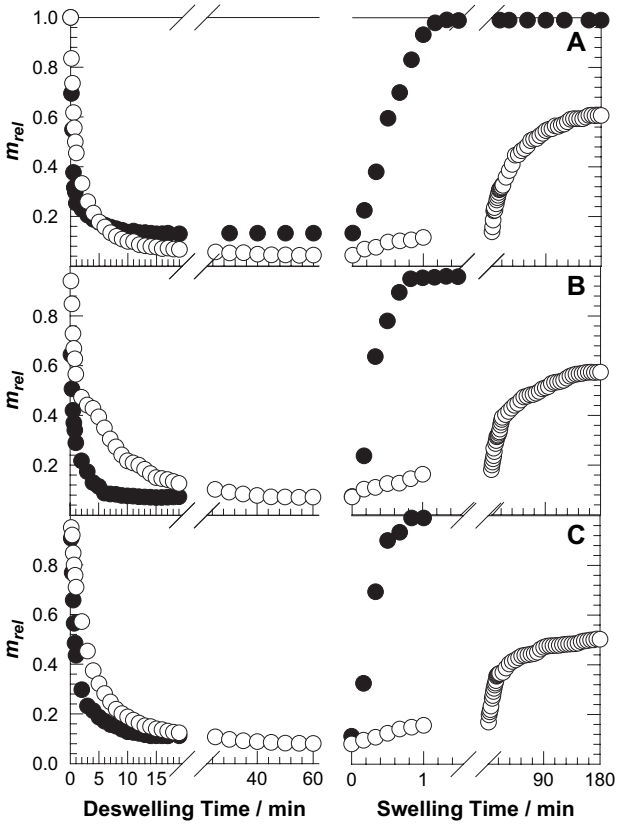

Fig. 8. Swelling and deswelling kinetics of PAAm hydrogels in water and in acetone, respectively, shown as the variation of the relative weight swelling ratio m_{rel} with the time of swelling or deswelling. (A): $C_o = 5$ w/v%, $X = 1/80$. (B): $C_o = 3$ w/v%, $X = 1/80$. (C): $C_o = 3$ w/v%, $X = 1/50$. The gel preparation temperature $T_{prep} = -18$ °C (●) and +21 °C (○).

again in water, it swelled instantaneously. The relatively slower rate of swelling of collapsed hydrogel in acetone compared to dry hydrogel (swelling times 1 min compared to a few seconds) seems to be related to the acetone molecules on the surface of the collapsed hydrogel sample, which decreases the solvating power of the liquid around the gel sample and slows down the swelling process. We conducted measurements of the swelling kinetics of all the hydrogels starting from their dry states. Similar results such as those in Fig. 9 were obtained for the hydrogels formed below −6 °C. All the hydrogels attain the equilibrium state in water within a few seconds. In contrast to this superfast swelling feature of the hydrogels formed from frozen monomer solutions, those prepared at room temperature ($T_{prep} = 21$ °C) required about 2–3 h to attain the equilibrium swollen state starting from the dry state (lower row in Fig. 9).

An interesting point of the present results appears if one compares the swelling rates of the hydrogels with those reported in the literature. Although several polymerization techniques were used before successfully to increase the deswelling rate of AAm-based hydrogels, the reswelling rate of collapsed or dry hydrogels cannot be improved; generally, such gels required tens to hundreds of minutes to attain the equilibrium swollen state in water [26–30]. This slow reswelling rate of the hydrogels reported in the literature is mainly

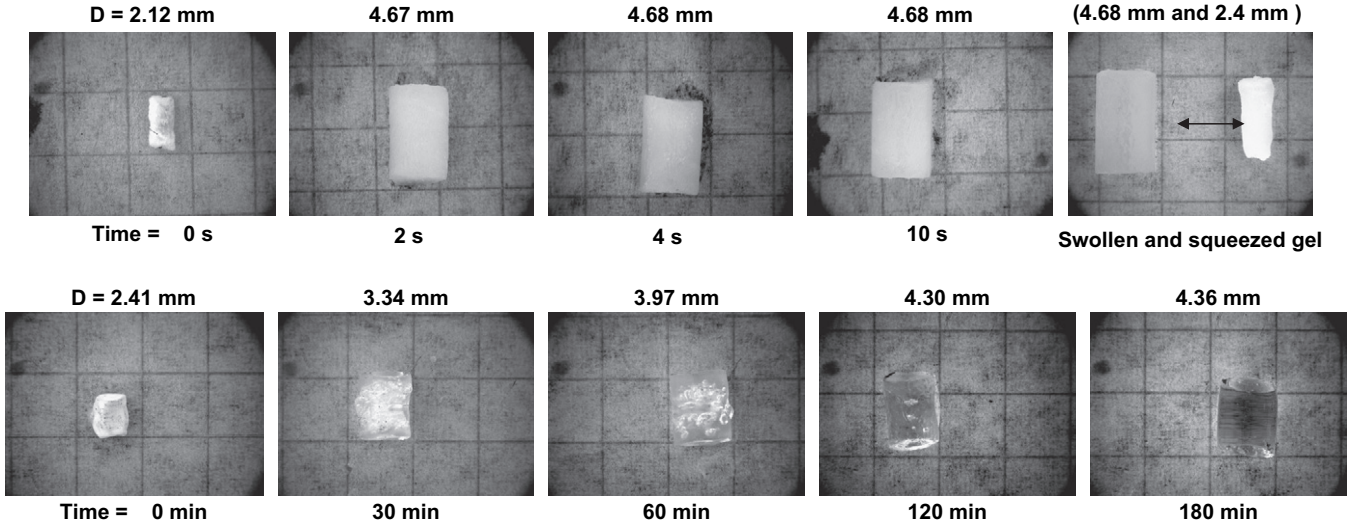

Fig. 9. A series of photographs taken during the swelling process of PAAm networks. The diameter of the gel samples together with the swelling times are given in the photographs. $C_o = 5$ w/v%, $X = 1/80$. $T_{prep} = -18$ °C (upper row) and +21 °C (lower row).

due to the collapse of their porous structure because of the cohesional forces between the solvated polymer chains. Here, however, we show that all the hydrogels formed below −6 °C swell within seconds. This is due to the stable pore structure which cannot collapse during drying or during deswelling, as well as due to the large water channels (pores) which enable diffusion of water in the hydrogel network.

4. Conclusion

The polymerization–crosslinking reactions conducted below −6 °C lead to the formation of macroporous PAAm hydrogels exhibiting superfast responsive properties. The gel preparation temperature T_{prep} together with the initial monomer concentration was found to be the key factor determining the porous structure of the networks. A maximum pore size was obtained if T_{prep} was set to −18 °C. Increasing monomer concentration decreased the size of the pores but increased the thickness of the pore walls so that the hydrogels prepared at higher monomer concentration exhibited good mechanical properties. The hydrogels formed below −6 °C exhibit superfast swelling and deswelling properties as well as reversible swelling–deswelling cycles in water and in acetone, respectively.

It should be noted that the experimental parameter T_{prep} of the present study is the temperature of the thermostated bath in which the reactions were carried out. Since the addition of the initiator APS into the monomer solution occurred at 0 °C, the reactions proceed non-isothermally from the moment of the APS addition to the moment when the temperature of the reaction system reaches to T_{prep}. For example, the freezing time of the reaction solution at $T_{prep} = -18$ °C was found to be 15 min, compared to the gelation time of 20 min. This means that gelation occurs non-isothermally during the cooling period from 0 to −18 °C. Here, in order to obtain reproducible freezing patterns, the reaction mixtures of the same volume and shape were used. The time period between the APS addition and the transfer of the reaction system into the thermostat was also accurately controlled. Experiments are in progress to provide an isothermal polymerization condition using addition of polymerization inhibitors into the reaction solutions.

Acknowledgements

This work was supported by the Scientific and Technical Research Council of Turkey (TUBITAK), TBAG – 105T246. M.V. Dinu is very grateful for the financial support by TUBITAK.

References

[1] Shibayama M, Tanaka T. Adv Polym Sci 1993;109:1.
[2] Tanaka T, Fillmore DJ. J Chem Phys 1979;70:1214.
[3] Oh KS, Oh JS, Choi HS, Bae YC. Macromolecules 1998;31:7328.
[4] Kaneko Y, Sakai K, Kikuchi A, Yoshida R, Sakurai Y, Okano T. Macromolecules 1995;28:7717.
[5] Okay O. Prog Polym Sci 2000;25:711.
[6] Worster MG, Wettlaufer JS. J Phys Chem B 1997;101:6132.
[7] Deville S, Saiz E, Nalla RK, Tomsia AP. Science 2006;311:515.
[8] Lozinsky VI. Russ Chem Rev 2002;71:489.
[9] Lozinsky VI, Plieva FM, Galaev IY, Mattiasson B. Bioseparation 2002; 10:163.
[10] Arvidsson P, Plieva FM, Lozinsky VI, Galaev IY, Mattiasson B. J Chromatogr A 2003;986:275.
[11] Ivanov RV, Babushkina TA, Lozinskii VI. Polym Sci Ser A 2005;47:791.
[12] Lozinskii VI, Kalinina EV, Grinberg VY, Grinberg VY, Chupov VV, Plate NA. Polym Sci Ser A 1997;39:1300.
[13] Ozmen MM, Okay O. Polymer 2005;46:8119.
[14] Sayil C, Okay O. Polymer 2001;42:7639.
[15] Treloar LRG. The physics of rubber elasticity. Oxford: University Press; 1975.
[16] Okoroafor EV, Newborough M, Highgate D, Augood P. J Phys D Appl Phys 1998;31:3120.
[17] Pissis P, Kyritsis A, Konsta AA, Daoukaki D. Colloids Surf A Physicochem Eng Aspects 1999;149:253.

[18] Okay O. Angew Makromol Chem 1987;153:125.
[19] Okay O. Polymer 1999;40:4117.
[20] Ilavsky M. Macromolecules 1982;15:782.
[21] Plieva FM, Karlsson M, Aguilar MR, Gomez D, Mikhalovsky S, Galaev IY. Soft Matter 2005;1:303.
[22] Ozmen MM, Okay O. J Macromol Sci A Pure Appl Chem 2006;43:1215.
[23] Franks F. Cryo-Letters 1986;7:207.
[24] Wolfe J, Bryant G, Koster KL. Cryo-Letters 2002;23:157.
[25] Watanabe K, Mizoguchi M. Cold Reg Sci Technol 2002;34:103.
[26] Kabra BG, Gehrke SH. Polym Commun 1991;32:322.
[27] Zhang X-Z, Yang Y-Y, Chung T-S, Ma K-X. Langmuir 2001;17:6094.
[28] Dogu Y, Okay O. J Appl Polym Sci 2006;99:37.
[29] Zhang X-Z, Zhuo R-X. Macromol Chem Phys 1999;200:2602.
[30] Zhuo R-X, Li W. J Polym Sci A Polym Chem 2003;41:152.